

1,2,3-Triazoles as Amide Bioisosteres: Discovery of a New Class of Potent HIV-1 Vif Antagonists

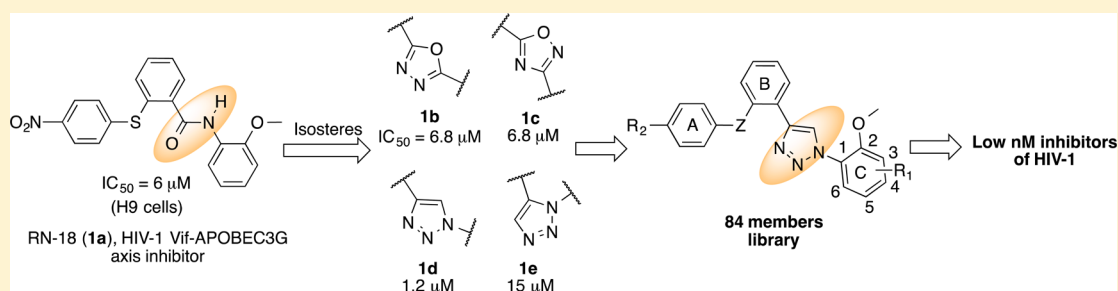
Idrees Mohammed,[†] Indrasena Reddy Kummetha,[‡] Gatikrushna Singh,[†] Natalia Sharova,[§] Gianluigi Lichinchi,^{†,‡} Jason Dang,[‡] Mario Stevenson,[§] and Tariq M. Rana^{*,†,‡}

[†]Program for RNA Biology, Sanford Burnham Prebys Medical Discovery Institute, La Jolla, California 92037, United States

[‡]Department of Pediatrics, University of California San Diego School of Medicine, 9500 Gilman Drive, MC 0762, La Jolla, California 92093 United States

[§]Division of Infectious Diseases, Miller School of Medicine, University of Miami, Miami, Florida 33136, United States

S Supporting Information



ABSTRACT: RN-18 based viral infectivity factor (Vif), Vif antagonists reduce viral infectivity by rescuing APOBEC3G (A3G) expression and enhancing A3G-dependent Vif degradation. Replacement of amide functionality in RN-18 ($IC_{50} = 6 \mu M$) by isosteric heterocycles resulted in the discovery of a 1,2,3-triazole, **1d** ($IC_{50} = 1.2 \mu M$). We identified several potent HIV-1 inhibitors from a **1d** based library including **Sax** ($IC_{50} = 0.01 \mu M$), **Sbx** ($0.2 \mu M$), **2ey** ($0.4 \mu M$), **5ey** ($0.6 \mu M$), and **6bx** ($0.2 \mu M$).

INTRODUCTION

Since the start of the AIDS epidemic in 1981, this disease has led to the death of >30 million people globally. Although the overall growth of the epidemic appears to be slowing, there were nearly three million new infections and an estimated 1.8 million AIDS-related deaths in 2010. Over the past two decades, more than 25 anti-HIV drugs have been developed targeting several different stages of the virus life cycle.¹ Among these agents, HIV-1 reverse transcriptase and protease inhibitors, when used in combinations in the highly active antiretroviral therapy (cART), have proven to be highly effective in reducing AIDS-related mortality throughout the world.² However, the development of drug resistance and toxic side effects associated with cART have created a need for more potent and less toxic therapies against other viral targets and host–virus interactions.³ In patients on effective cART, plasma viremia can be suppressed to below detectable levels for extended intervals and the ability of cART to sustain this aviremic state has promoted the view that cART is fully suppressive and effectively stops all ongoing viral replication. However, there is rapid recrudescence of plasma viremia upon treatment interruption, regardless of the prior interval of viral suppression, indicating the presence of long-lived viral reservoirs that maintain viral persistence in the face of cART.

Therefore, new antiviral regimens are needed to eliminate these viral reservoirs.

The HIV-1 accessory protein viral infectivity factor, Vif, is essential for in vivo viral replication.^{4,5} HIV-1 Vif protein targets an innate antiviral human DNA-editing enzyme, APOBEC3G (A3G),⁶ which inhibits replication of retroviruses.⁷ A3G catalyzes critical hypermutations in the viral DNA and acts as an innate weapon against retroviruses.⁵ Cells that express A3G are “non-permissive” in that viral replication is absolutely dependent on a functional Vif. In contrast, HIV-1 replication is Vif-independent in host cells that do not express A3G (permissive cells). Because HIV-1 Vif has no known cellular homologues, this protein represents an extremely attractive, yet unrealized, target for antiviral intervention.

The RN-18 based class of small molecule Vif antagonists reduce viral infectivity by enhancing A3G-dependent Vif degradation, increasing A3G incorporation into virions, and enhancing cytidine deamination of the viral genome.^{8–10} RN-18 (**1a**) exhibits IC_{50} values of 4.5 and 6 μM in CEM cells and H9 cells (nonpermissive cells), respectively. RN-18 does not inhibit viral infectivity in MT4 cell line (permissive cells) even at 100 μM , demonstrating that these inhibitors are Vif-specific.

Received: February 17, 2016

These findings provided the proof of concept that the HIV-1 Vif-A3G axis is a valid target for developing small molecule based new therapies for AIDS or for enhancing innate immunity against viruses.

We faced two major challenges for further development of RN-18 based Vif antagonists as clinical candidates: (a) potency and (b) metabolic stability. To address these questions, we planned to explore isosteric replacement of the amide functionality in RN-18. We reasoned to test a series of conformationally restricted, biocompatible and metabolically stable isosteric heterocyclic systems. Next, on the basis of the activity, we would select and develop a suitable bioisosteric series to improve the both activity and pharmacological profiles.

RESULTS AND DISCUSSION

In this communication, we describe the successful identification of potent bioisosteric analogues of RN-18. Initially, we designed and synthesized four test molecules by substituting the amide functionality in the lead molecule with isosteric heterocyclic systems such as 1,3,4-oxadiazole¹² **1b**, 1,2,4-oxadiazole¹³ **1c**, 1,4-disubstituted-1,2,3-triazole¹⁴ **1d**, and 1,5-disubstituted-1,2,3-triazole¹⁵ **1e** (Figure 1).

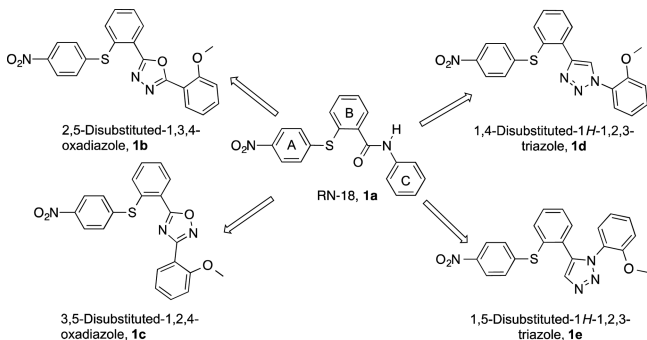
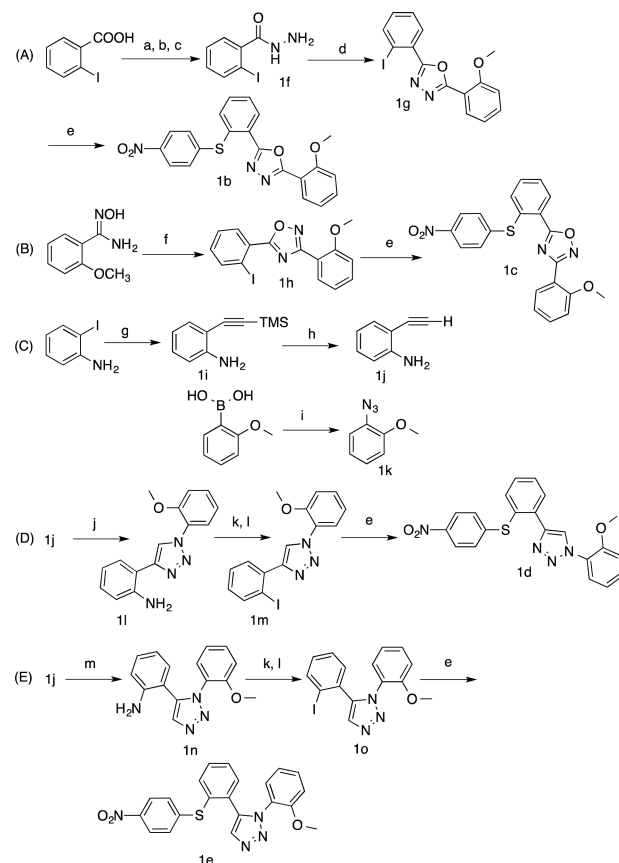


Figure 1. Amide bioisosteres of **1a**, RN-18.

1,3,4-Oxadiazole **1b** was synthesized with the coupling of hydrazine and 2-iodobenzoic acid (Scheme 1A). The one pot coupling involves the formation of in situ methyl ester of 2-iodobenzoic acid, which was later refluxed in the presence of hydrazine hydrate to obtain the benzohydrazide derivative **1f** quantitatively. Benzohydrazide **1f** was later reacted with *o*-anisic acid in refluxing phosphoryl chloride, leading to the formation of iodo intermediate 1,3,4-oxadiazole **1g**. Intermediate **1g** was reacted with 4-nitrothiophenol under copper(I) catalyzed S-arylation conditions,¹⁶ leading to the formation of **1b**. Synthesis of 1,2,4-oxadiazole **1c** was started (Scheme 1B) with the coupling between the commercially available *N*'-hydroxy-2-methoxybenzimidamide, leading to the formation of the iodo intermediate 1,2,4-oxadiazole **1h**. S-Arylation of **1h** with 4-nitrothiophenol under copper(I) catalytic conditions led to the formation of 3,5-disubstituted-1,2,4-oxadiazole, **1c**.

Synthesis of 1,4-disubstituted-1,2,3-triazole analogue **1d** required two synthons, 2-ethynylaniline **1j** and 1-azido-2-methoxybenzene **1k** (Scheme 1C). 2-Iodoaniline was reacted with trimethylsilylacetylene under Sonogashira reaction conditions catalyzed by bis(triphenylphosphine)palladium chloride in the presence of triethylamine base and copper iodide as cocatalyst,¹⁸ leading to the formation of TMS protected ethynylaniline **1i**, which was deprotected using sodium

Scheme 1. Synthesis of Isosteric Analogues of RN-18^a



^aReagents and conditions: (a) SOCl_2 , cat. DMF, benzene, 80 °C, 2 h; (b) CH_3OH , TEA, 0 °C–rt, 2 h; (c) $\text{NH}_2\text{NH}_2 \cdot \text{H}_2\text{O}$, 80 °C, 3 h; (d) *o*-anisic acid, POCl_3 , 110 °C, 8 h; (e) 4-nitrothiophenol, K_2CO_3 , 5 mol %, CuI, DMF, 110 °C, 8 h; (f) 2-iodobenzoic acid, DCC, DMF, rt to 100 °C, 8 h; (g) trimethylsilyl acetylene, 1 mol % $\text{PdCl}_2(\text{PPh}_3)_2$, 1 mol % CuI, NET_3 , rt, 12 h; (h) NaOH (aq), ethanol/THF (1:1), rt, 1 h; (i) NaN_3 , 10 mol % $\text{CuSO}_4 \cdot 5\text{H}_2\text{O}$, CH_3OH , rt, 8 h; (j) **1k**, 5 mol % $\text{CuSO}_4 \cdot 5\text{H}_2\text{O}$, 10 mol % Na ascorbate, *t*-BuOH/ H_2O (1:1), rt, overnight; (k) NaNO_2 , 5 N HCl, –10 to –5 °C, 2 h; (l) KI, –10 to –5 °C, 8 h; (m) **1k**, 1 mol % $\text{Cp}^*\text{RuCl}(\text{PPh}_3)_2$, benzene, 80 °C, 3 h.

hydroxide, affording the required synthon 2-ethynylaniline **1j**. Azide **1k** was synthesized by following a Cham-Lam type of coupling between 2-methoxyphenylboronic acid and sodium azide catalyzed by copper sulfate at room temperature in methanol.¹⁹ Copper-catalyzed click reaction²⁰ between alkyne **1j** and azide **1k** generated triazole amine **1l** quantitatively in *t*-butanol/water (Scheme 1D). Triazole amine **1l** was diazotized using sodium nitrite in 5 N HCl around –10 °C and concomitantly converted to iodotriazole **1m** by reacting with potassium iodide. Copper(I) catalyzed S-arylation of iodo-triazole **1m** using 4-nitrothiophenol in DMF solvent and potassium carbonate led to the synthesis of **1d**, IMA-53. 1,5-Disubstituted-1,2,3-triazole **1e** analogue was synthesized initially by reacting alkyne **1j** and azide **1k** under ruthenium catalyzed click chemistry conditions using $\text{Cp}^*\text{RuCl}(\text{PPh}_3)_2$ catalyst in benzene at 80 °C,²¹ leading to the formation of amine **1n** (Scheme 1E). Diazotization, iodination (**1o**), and S-arylation reaction sequences afforded 1,5-disubstituted-1,2,3-triazole **1e**.

The antiviral activities of the four synthesized RN-18 analogues were measured against wild-type HIV-1 both in

nonpermissive H9 and permissive MT-4 cells (see details of methods in [Supporting Information \(SI\)](#)). In all the antiviral activity measurements, RN-18 (**1a**) was used as a positive control and the cells cultured without any inhibitor served as a negative control. The IC_{50} values of the bioisosteric analogues of RN-18 are presented in [Table 1](#). Both 1,3,4-oxadiazole **1b**

Table 1. IC_{50} Values of the Isoosteric Analogues of RN-18

| compd | antiviral activity (IC_{50} μ M) | |
|-------------------|---|-----------------|
| | H9 cells | MT4 cells |
| 1a , RN-18 | 6 | NA ^a |
| 1b | 6.8 | 50 |
| 1c | 6.8 | NA ^a |
| 1d | 1.2 | NA ^a |
| 1e | 15 | 25 |

^aNA = no activity even at 50 μ M conc.

(IC_{50} = 6.8 μ M) and 1,2,4-oxadiazole **1c** (IC_{50} = 6.8 μ M) based analogues exhibited cell-based antiviral activity in the nonpermissive H9 cells similar to the lead molecule RN-18 (IC_{50} = 6 μ M). Interestingly, 2,5-disubstituted-1,3,4-oxadiazole **1b** showed nonspecific antiviral activity with IC_{50} of 50 μ M in permissive MT4 cells, whereas the 1,4-disubstituted-1,2,3-triazole based analogue **1d** exhibited remarkably better anti-HIV activity (IC_{50} = 1.2 μ M in H9 cells) and specificity (no activity in MT4 cells). On the contrary, 1,5-disubstituted-1,2,3-triazole **1e** analogue exhibited comparatively lesser potency (IC_{50} = 15 μ M in H9 cells) with nonspecific activity in the permissive cells (IC_{50} = 25 μ M in MT4 cells).

Next, to determine the mechanism of these bioisosteres of RN-18, we analyzed Vif degradation and rescue of A3G levels in the presence of these compounds and compared with RN-18. 293FT cells coexpressing hemagglutinin (HA)-tagged A3G and green fluorescent protein (GFP)-tagged Vif or Δ Vif were treated with various compounds (50 μ M) for 16 h (see [SI, methods details](#)). The cell extracts were then analyzed by immunoblotting with anti-HA-A3G, anti-GFP-Vif, and anti-GAPDH antibodies ([Figure 2](#)). All the bioisostere analogues of RN-18 resulted in restoring A3G levels in the presence of Vif and down-regulated Vif expression, indicating that these analogues (**1b**, **1c**, **1d**, and **1e**) are capable of antagonizing Vif function similar to RN-18. However, analogues **1b** and **1e** also exhibited some nonspecific activity ([Table 1](#)).

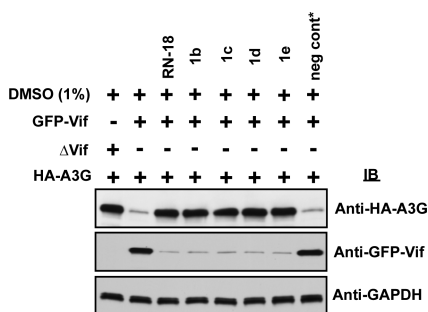
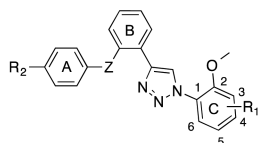


Figure 2. Bioisosteric analogues of RN-18 enhance A3G levels and reduce Vif expression. 293FT cells coexpressing HA-tagged A3G and GFP-tagged Vif or Δ Vif were incubated in the presence (50 μ M) or in the absence of the compounds for 16 h. See [SI](#) for the structure of negative control (**8s**). Anti-HA-A3G, anti-GFP-Vif, and anti-GAPDH antibodies were used for immunoblotting (see [SI](#) for details).

These observations were well in-line with the structural similarities in the 3D orientations except the 1,5-disubstituted-1,2,3-triazole **1e**, which has a twisted structure (see [SI, crystallographic data](#)). 1,3,4-Oxadiazole and 1,2,4-oxadiazole heterocyclic systems have both planarity and dipole moment similar to the amide functionality. Similarly, 1,4-disubstituted and 1,5-disubstituted 1,2,3-triazoles possess strong dipole moment beside having better H-bond accepting (N(2) and N(3)) and H-bond donating (triazole C(5)-H) capacity than an amide functionality.²² However, in the current biochemical context, 1,4-disubstituted-1,2,3-triazole **1d** analogue showed both improved antiviral activity (IC_{50} = 1.2 μ M) and selectivity (no activity in MT4 cells).

Having discovered **1d** as a potent and specific inhibitor of Vif-A3G axis, we decided to optimize the analogue to generate a new class of anti-HIV drug candidates for clinical development. We designed and synthesized an 84-membered library using a parallel format exploring various substitution patterns in ring-A, ring-C, and bridge A–B in the **1d** structure ([Table 2](#)). In this direction, the synthetic scheme for **1d** ([Scheme 1D](#)) was followed. Synthetic schemes (see [SI, Schemes 1S–6S](#)), experimental procedures, and characterization data of all the 84 members of the library are given in the [SI](#). Antiviral activities of the library were determined against wild-type HIV-1 both in nonpermissive H9 and permissive MT-4 cells. The IC_{50} values for important compounds are presented in [Table 2](#). Antiviral activities of the complete library is given in the [SI, Table 1S](#). None of the 84 compounds exhibited antiviral activities at 50 μ M in nonpermissive MT4 cells indicating the requirement of Vif for their function, which is quite remarkable. Further analysis of a selective set of potent compounds showed dose-dependent inhibition of HIV-1 in H9 cells with no significant toxicity at 50 μ M as measured by MTS cell viability assays ([SI, Figures 1S,2S](#)).

For a few selected compounds (**2dx**, **2ey**, **2gy**, **5ax**, **5bx**, **5gy**, and **5ey**), we then determined whether the analogues could upregulate A3G and downregulate Vif in a manner similar to RN-18 and **1d**. Immunoblots for A3G and Vif in the presence of compounds are shown in [Figure 3](#), which clearly showed that the new inhibitors exert the anti-HIV activity via the same mechanism as observed for RN-18 and **1d**. Of the 84 members library, about 30 compounds inhibited HIV-1 with IC_{50} values in the range of 0.01–5 μ M in the nonpermissive H9 cells. Among them, the **5ax** exhibited the most potent activity with an IC_{50} of 10 nM, which is about 1000-fold more potent than the original lead molecule, RN-18. Similarly, **2ey**, **5bx**, **5ey**, and **6bx** exhibited IC_{50} values in the range of 0.2–0.6 μ M and **2ax**, **2dx**, **2ex**, **2fx**, **3ax**, **3dx**, **3fx**, **3fy**, **5ay**, **6ex**, **6fx**, **6ey**, and **6fy** in the range of 1–3 μ M. Three water-soluble choline salts **2gy**, **4gy**, and **5gy** exhibited IC_{50} values of 0.2, 0.7, and 0.5 μ M, respectively. Overall, the SAR of the library showed striking sensitivity toward the three variables (Z-bridge, R₁ and R₂ substituents) tested in this study. Among various SAR findings, few of the noteworthy ones are in general sulfide (–S–) as bridge Z exhibited overall better activity compared with sulfone (–SO₂–) bridge (in the case of RN-18 sulfone derivative showed better activity).⁹ However, sulfones (–SO₂–) showed better activities when the R₂ substituent was an amino group. This study has found replacements such as –COOCH₃, –COOH, –CF₃, –NH₂, and –choline carboxylate for the nitro functionality in RN-18.

Table 2. IC₅₀ Values of the Library

R₁ = H (2), 3-OCH₃ (3), 4-OCH₃ (4), 5-OCH₃ (5), 6-OCH₃ (6), 6-F (7)
 R₂ = NO₂ (a), COOCH₃ (b), OCH₃ (c), CF₃ (d), NH₂ (e), COOH (f)
 Choline carboxylate (g)
 Z = S (x), SO₂ (y)

| compd | Z | R ₁ | R ₂ | antiviral activity (IC ₅₀ μM) H9 Cells |
|----------|-----------------|--------------------|--------------------|--|
| 2ax (1d) | S | H | NO ₂ | 1.2 |
| 2dx | S | H | CF ₃ | 2.6 |
| 2ex | S | H | NH ₂ | 2.5 |
| 2fx | S | H | COOH | 1.0 |
| 2ay | SO ₂ | H | NO ₂ | 13.8 |
| 2cy | SO ₂ | H | OCH ₃ | 4.3 |
| 2dy | SO ₂ | H | CF ₃ | 4.8 |
| 2ey | SO ₂ | H | NH ₂ | 0.4 |
| 2fy | SO ₂ | H | COOH | 8.2 |
| 2gy | SO ₂ | H | CC ^a | 0.2 |
| 3ax | S | 3-OCH ₃ | NO ₂ | 1.1 |
| 3bx | S | 3-OCH ₃ | COOCH ₃ | 8 |
| 3dx | S | 3-OCH ₃ | CF ₃ | 1.9 |
| 3fx | S | 3-OCH ₃ | COOH | 2.8 |
| 3gx | S | 3-OCH ₃ | CC ^a | 4.3 |
| 3by | SO ₂ | 3-OCH ₃ | COOCH ₃ | 4.7 |
| 3ey | SO ₂ | 3-OCH ₃ | NH ₂ | 12.4 |
| 3fy | SO ₂ | 3-OCH ₃ | COOH | 1.4 |
| 4fx | S | 4-OCH ₃ | COOH | 7.1 |
| 4dy | SO ₂ | 4-OCH ₃ | CF ₃ | 12 |
| 4gy | SO ₂ | 4-OCH ₃ | CC ^a | 0.7 |
| 5ax | S | 5-OCH ₃ | NO ₂ | 0.01 |
| 5bx | S | 5-OCH ₃ | COOCH ₃ | 0.2 |
| 5fx | S | 5-OCH ₃ | COOH | 4.5 |
| 5ay | SO ₂ | 5-OCH ₃ | NO ₂ | 1.0 |
| 5by | SO ₂ | 5-OCH ₃ | COOCH ₃ | 4.6 |
| 5ey | SO ₂ | 5-OCH ₃ | NH ₂ | 0.6 |
| 5gy | SO ₂ | 5-OCH ₃ | CC ^a | 0.5 |
| 6bx | S | 6-OCH ₃ | COOCH ₃ | 0.2 |
| 6ex | S | 6-OCH ₃ | NH ₂ | 1.5 |
| 6fx | S | 6-OCH ₃ | COOH | 1.9 |
| 6ey | SO ₂ | 6-OCH ₃ | NH ₂ | 1.5 |
| 6fy | SO ₂ | 6-OCH ₃ | COOH | 1.2 |
| 7ax | S | 6-F | NO ₂ | 3.9 |
| 7bx | S | 6-F | COOCH ₃ | 7.8 |
| 7fx | S | 6-F | COOH | 4.9 |
| 7ey | SO ₂ | 6-F | NH ₂ | 15 |

^aCholine carboxylate.

CONCLUSION

In summary, this study reports three major findings: (a) 1,4-disubstituted-1,2,3-triazole system is a suitable bioisostere in the RN-18 context, (b) discovery of a new class of potent Vif antagonists as preclinical candidates for novel AIDS therapy, and (c) generation of potent chemical modulators for perturbing and understanding the Vif-A3G axis. Further optimization of 1,4-disubstituted-1,2,4-oxadiazole, 1c, and preclinical studies for the selected 1,4-disubstituted-1,2,3-triazole based Vif antagonists are in progress.

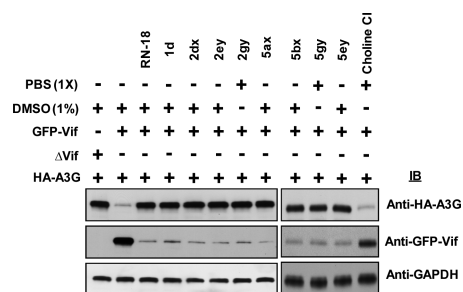


Figure 3. Triazole-based Vif antagonist small molecules enhance A3G levels and reduce Vif expression. 293FT cells coexpressing HA-tagged A3G and GFP-tagged Vif or ΔVif were incubated in the presence (50 μM) or in the absence of the compounds for 16 h. Choline chloride was used as a negative control.

EXPERIMENTAL SECTION

Details of general procedures and materials are described in the SI. Parallel synthesis was performed using Carousel 6 (Radleys Discovery Technologies). ¹H and ¹³C NMR spectra were recorded using a 400 MHz Jeol JNM-ECS spectrometer (equipped with a 5 mm proton/multifrequency autotune and an auto sample changer) with trimethylsilane (TMS) as the internal reference. The spectra are reported in ppm on the δ scale. ESI MS was performed on Waters micromass model ZQ 4000 using methanol. HRMS was performed on Agilent Technologies 6224A MS-TOF. Purity of the tested compounds was determined using Waters 2695 module HPLC equipped with Waters 996 photodiode detector at 254 nm. Purity of the final compounds mentioned in Tables 1 and 2 was found to be ≥95% in HPLC. X-ray structural determination was performed at UCSD facility using Bruker diffractometer with CCD detectors and low-temperature cryostats.

2-Iodobenzohydrazide (1f). A suspension of 2-iodobenzoic acid (2.48 g, 10 mmol) and SOCl₂ (1.43 g, 12 mmol) in dry benzene 25 mL was refluxed for about 2 h at 80 °C in the presence of catalytic DMF (2 drops). Benzene and excess SOCl₂ were removed under reduced pressure. The residue obtained was slowly treated with methanol (25 mL) at 0 °C, and triethylamine (5 mL) was added followed by stirring at room temperature for 2 h. To the above mixture hydrazine hydrate (1.0 g, 20 mmol) was added dropwise, and the mixture was refluxed at 80 °C for about 3 h. TLC showed the completion of the reaction. The reaction mixture was dried under reduced pressure and extracted with AcOEt (2 × 25 mL). The organic extract was sequentially treated with saturated solution of NaHCO₃, brine, and anhydrous Na₂SO₄. Flash column chromatography using AcOEt:hexane (1:1) afforded colorless amorphous solid 1f (1.99 g, 76% yield).

2-(2-Iodophenyl)-5-(2-methoxyphenyl)-1,3,4-oxadiazole (1g). A 50 mL round-bottom flask was discharged with *o*-anisic acid (0.30 g, 2 mmol) and benzohydrazide 1f (0.52 g, 2 mmol) followed by the addition of POCl₃ (8 mL). The suspension was refluxed at 110 °C for 8 h until TLC showed depletion of the starting materials. The reaction mixture was poured into cold saturated solution of K₂CO₃ followed by extraction with AcOEt (2 × 25 mL). The organic extract was treated with saturated solution of NaHCO₃ and dried over anhydrous Na₂SO₄. TLC (AcOEt:hexane, 1:1) showed two new spots with almost equal intensity. Flash chromatographic separation of the upper spot using AcOEt:hexane (1:1) afforded colorless amorphous solid 1g (0.41 g, 55% yield).

2-(2-Methoxyphenyl)-5-(2-((4-nitrophenyl)thio)phenyl)-1,3,4-oxadiazole (1b). *S*-Aylation procedure described for the synthesis of 1d (see below) was followed for the synthesis of 1b using the intermediate 1g and 4-nitrothiophenol as starting materials. Flash chromatography using AcOEt:hexane (1:3) afforded the compound as a light-yellow amorphous solid (0.219 g, 82% yield), which was crystallized using a mixture of DCM and methanol to afford light-yellow crystalline 1b.

5-(2-Iodophenyl)-3-(2-methoxyphenyl)-1,2,4-oxadiazole (1h). A solution of 2-iodobenzoic acid (0.99 g, 4 mmol) in 15 mL of dry DMF was cooled to 0 °C followed by the addition of dicyclohexylcarbodiimide (1.24 g, 6.0 mmol) under N₂ atmosphere, and the reaction mixture was stirred for an hour at 0 °C. To the above mixture was added commercially available *N'*-hydroxy-2-methoxybenzimidamide (0.664 g, 4 mmol) and stirred for 30 min at 0 °C. Then for 3 h stirring was continued at room temperature. Gradually, the reaction mixture was heated up to 110 °C and kept for 8 h. The reaction mixture was later poured into ice-cold water and diluted using AcOEt (20 mL). Dicyclohexylurea crystals formed were separated by filtration. Filtrate organic layer was treated with saturated solution of K₂CO₃, brine, and anhydrous Na₂SO₄. Flash chromatography using AcOEt:hexane (1:3) afforded the required **1h** as a colorless amorphous solid (1.2 g, 80% yield).

3-(2-Methoxyphenyl)-5-(2-((4-nitrophenyl)thio)phenyl)-1,2,4-oxadiazole (1c). *S*-Aylation procedure described for the synthesis of **1d** was followed for the synthesis of **1c** using the intermediate **1h** and 4-nitrothiophenol as starting materials. Flash chromatography using AcOEt:hexane (1:3) afforded the compound as a light-yellow amorphous solid (0.225 g, 84% yield), which was crystallized using a mixture of DCM and methanol to afford light-yellow crystalline **1c**.

2-((Trimethylsilyl)ethynyl)aniline (1i). In a dry 500 mL two-necked round-bottom flask, 2-iodoaniline (25.0 g, 0.114 mol) was dissolved in 250 mL of deoxygenated triethylamine. To this solution, PdCl₂(PPh₃)₂ catalyst (0.8 g, 1.14 mmol, 1 mol %) and copper(I) iodide cocatalyst (0.217 g, 1.14 mmol, 1 mol %) were added. The mixture was stirred for 15 min at room temperature under N₂ pressure. To this mixture, trimethylacetylene (11.21 g, 0.114 mol) was added and stirred for 12 h at room temperature. Triethylamine was removed under reduced pressure to get a crude viscous residue. The residue was dissolved in AcOEt (250 mL) treated with saturated brine and Na₂SO₄ and adsorbed on neutral alumina. Flash column chromatography using AcOEt:hexane (1:9) afforded pale-yellow liquid **1i** (18.37 g, 85% yield).

2-Ethynylaniline (1j). A 1 M aqueous solution of NaOH (2.64 g, 65.95 mmol, 1.2 equiv) was added to a solution of 2-ethynylaniline **1i** (18.0 g, 54.96 mmol, 1 equiv) dissolved in 200 mL of ethanol/THF (1:1). Stirring was continued at room temperature for about 1 h until TLC showed complete disappearance of the starting material. Organic solvents were evaporated under reduced pressure, and the residue was diluted by adding 50 mL of deionized water and extracted with DCM (2 × 100 mL). Organic extractions were dried over brine and Na₂SO₄ and adsorbed on neutral alumina. Flash column chromatography using AcOEt:hexane (1:4) afforded colorless pale-yellow liquid **1j** (6.18 g, 96% yield).

1-Azido-2-methoxybenzene (1k). To a solution of 2-methoxyphenylboronic acid (1.52 g, 10 mmol) in 20 mL of methanol, sodium azide (0.78 g, 12.0 mmol) was added and stirred. To this mixture CuSO₄·5H₂O (0.249 g, 1 mmol, 10 mol %) was added and stirred at room temperature for about 8 h until TLC showed completion of the reaction. Methanol was removed under reduced pressure, and the residue was treated with saturated solution of sodium bicarbonate followed by extraction with DCM (2 × 20 mL). Organic extractions were dried over anhydrous Na₂SO₄ and adsorbed on silica gel. Flash column chromatography using AcOEt:hexane (1:9) afforded colorless dark-brown liquid **1k** (1.34 g, 90% yield).

2-(1-(2-Methoxyphenyl)-1*H*-1,2,3-triazol-4-yl)aniline (1l). 2-Ethynylaniline **1j** (0.234 g, 2 mmol) and 1-azido-2-methoxybenzene **1k** (0.298 g, 2 mmol) were dissolved in 10 mL of a mixture of *tert*-butanol and deionized water (1:1) in a 50 mL round-bottom flask. To the stirred solution sodium ascorbate (39.62 mg, 0.2 mmol, 10 mol %) and CuSO₄·5H₂O (24.97 mg, 0.1 mmol, 5 mol %) were added. Stirring was continued overnight until TLC showed the completion of the reaction. *t*-Butanol was removed under reduced pressure, and the viscous residue was extracted with DCM (2 × 10 mL). The combined organic extractions were treated with saturated brine and anhydrous Na₂SO₄ followed by adsorption on neutral alumina. Flash chromatog-

raphy using AcOEt:hexane (1:3) afforded the triazole amine **1l** as a light-brown amorphous solid (0.467 g, 88% yield).

4-(2-Iodophenyl)-1-(2-methoxyphenyl)-1*H*-1,2,3-triazole (1m). In a 50 mL round-bottom flask triazole amine **1l** (0.266 g, 1 mmol) was dissolved in 10 mL of 5 N HCl at 0 °C and stirred for 30 min. Sodium nitrite (82.8 mg, 1.2 mmol) dissolved in a minimum amount of water was added dropwise to the above mixture at -10 °C. Stirring was continued at -10 °C for a period of 2 h to get diazonium salt *in situ*. Urea (~50 mg) was added to the reaction mixture to remove any excess nitrous acid generated *in situ*. In a separate beaker, KI (0.249 g, 1.5 mmol) was dissolved in 5 mL of deionized water and kept at -5 °C. To this solution of KI was added the diazonium hydrochloride solution drop-by-drop using dropping funnel. After addition, stirring was continued for a period of 8 h at room temperature. The reaction mixture was later diluted with 20 mL of AcOEt and 10 mL of deionized water. Small amount of iodine liberated in the reaction was quenched by the addition of sodium dithionite. Organic layer was separated and was sequentially treated with saturated NaHCO₃, saturated brine, and anhydrous Na₂SO₄ followed by adsorption on silica gel. Flash chromatography using AcOEt:hexane (1:3) afforded **1m** as a colorless amorphous solid (0.293 g, 78% yield).

1-(2-Methoxyphenyl)-4-(2-((4-nitrophenyl)thio)phenyl)-1*H*-1,2,3-triazole (1d). In a dry 25 mL two-neck round-bottom flask, iodo triazole **1m** (0.25 g, 0.66 mmol, 1 equiv) was dissolved in 5 mL of dry DMF followed by the addition of anhydrous K₂CO₃ (0.110 g, 0.79 mmol, 1.2 equiv) and catalyst copper iodide (6.31 mg, 0.033 mmol, 5 mol %). The resulting mixture was stirred for 10 min under N₂ pressure. 4-Nitrothiophenol (0.123 g, 0.79 mmol, 1.2 equiv) dissolved in 2 mL of anhydrous DMF was added to the above reaction mixture and stirred at 110 °C for 8 h. The reaction mixture was poured then into ice-cold water followed by extraction with AcOEt (2 × 10 mL). Organic extractions were treated sequentially with saturated K₂CO₃ solution and anhydrous Na₂SO₄. The dried organic extract was adsorbed on silica gel and flash chromatography using AcOEt:hexane (1:3) afforded **1d** as a light-yellow amorphous solid (0.219 g, 82% yield). The amorphous solid was crystallized using a mixture of DCM and methanol to afford light-yellow crystalline **1d**.

2-(1-(2-Methoxyphenyl)-1*H*-1,2,3-triazol-5-yl)aniline (1n). 2-Ethynylaniline **1j** (0.234 g, 2 mmol) and 1-azido-2-methoxybenzene **1k** (0.298 g, 2 mmol) were dissolved in 10 mL of anhydrous benzene. To the above stirred solution, Cp*RuCl(PPh₃)₂ (15.90 mg, 0.02 mmol, 1 mol %) catalyst was added and the reaction mixture was refluxed at 80 °C under N₂ pressure for 3 h until TLC showed the completion of the reaction. Benzene was removed under reduced pressure, and the viscous residue was extracted with DCM (2 × 10 mL). The combined extractions were dried over Na₂SO₄ followed by adsorption on neutral alumina. Flash chromatography using AcOEt:hexane (2:3) afforded **1n** as a brown amorphous solid (0.488 g, 92% yield).

5-(2-Iodophenyl)-1-(2-methoxyphenyl)-1*H*-1,2,3-triazole (1o). Procedure described for the synthesis of intermediate **1m** was followed using **1n** as starting material to afford colorless amorphous solid **1o** (0.282 g, 75% yield).

1-(2-Methoxyphenyl)-5-(2-((4-nitrophenyl)thio)phenyl)-1*H*-1,2,3-triazole (1e). *S*-Aylation procedure described for the synthesis of **1d** was followed for the synthesis of **1e** using the intermediate **1o** and 4-nitrothiophenol as starting materials. Flash chromatography using AcOEt:hexane (1:3) afforded the compound as a light-yellow amorphous solid (0.227 g, 85% yield), which was crystallized using a mixture of DCM and methanol to afford light-yellow crystalline **1e**.

■ ASSOCIATED CONTENT

Supporting Information

The Supporting Information is available free of charge on the ACS Publications website at DOI: 10.1021/acs.jmedchem.6b00247.

Details of general procedures, synthetic schemes, characterization data, antiviral activities, and immunoblotting experiments (PDF)
Molecular formula strings (CSV)

AUTHOR INFORMATION

Corresponding Author

*Phone: 858-246-1100. Fax: 858-246-1600. E-mail: trana@ucsd.edu.

Author Contributions

The manuscript was written through contributions of all authors. All authors have given approval to the final version of the manuscript.

Notes

The authors declare no competing financial interest.

ACKNOWLEDGMENTS

This work was supported in part by grants from the NIH MH 100942 and DA 039562.

ABBREVIATIONS USED

APOBEC3G (A3G), apolipoprotein B mRNA editing enzyme catalytic polypeptide like 3G; CC, choline carboxylate; DCM, dichloromethane; DMF, dimethylformamide; TMS, trimethylsilyl; TLC, thin-layer chromatography; THF, tetrahydrofuran; Vif, viral infectivity factor

REFERENCES

- (1) Mehellou, Y.; Clercq, E. D. Twenty-six years of anti-HIV drug discovery: where do we stand and where do we go? *J. Med. Chem.* **2010**, *53*, 521–538.
- (2) Thompson, M. A.; Aberg, J. A.; Cahn, P.; Montaner, J. S. G.; Rizzardini, G.; Telenti, A.; Gatell, J. M.; Günthard, H. F.; Hammer, S. M.; Hirsch, M. S.; Jacobsen, D. M.; Reiss, P.; Richman, D. D.; Volberding, P. A.; Yeni, P.; Schooley, R. T. Antiretroviral treatment of adult HIV infection: 2010 recommendations of the International AIDS Society-USA panel. *JAMA* **2010**, *304*, 321–333.
- (3) Volderbing, P. A.; Deeks, S. G. Antiretroviral therapy and management of HIV injection. *Lancet* **2010**, *376*, 49–62.
- (4) Gabuzda, D. H.; Lawrence, K.; Langhoff, E.; Terwilliger, E.; Dorfman, T.; Haseltine, W. A.; Sodroski, J. Role of vif in replication of human immunodeficiency virus type 1 in CD4+ T lymphocytes. *J. Virol.* **1992**, *66*, 6489–6495.
- (5) Strelbel, K.; Daugherty, D.; Clouse, K.; Cohen, D.; Folks, T.; Martin, M. A. The HIV A (*sor*) gene product is essential for virus infectivity. *Nature* **1987**, *328*, 728–730.
- (6) Sheehy, A. M.; Gaddis, N. C.; Choi, J. D.; Malim, M. H. Isolation of a human gene that inhibits HIV-1 infection and is suppressed by the viral Vif protein. *Nature* **2002**, *418*, 646–650.
- (7) Malim, M. H.; Bieniasz, P. D. HIV restriction factors and mechanisms of evasion. *Cold Spring Harbor Perspect. Med.* **2012**, *2*, a006940.
- (8) Ali, A.; Wang, J.; Nathans, R. S.; Cao, H.; Sharova, N.; Stevenson, M.; Rana, T. M. Synthesis and structure-activity relationship studies of HIV-1 viron infectivity factor (Vif) inhibitors that block viral replication. *ChemMedChem* **2012**, *7*, 1217–1229.
- (9) Mohammed, I.; Parai, M. K.; Jiang, X.; Sharova, N.; Singh, G.; Stevenson, M.; Rana, T. M. SAR and lead optimization of an HIV-1 Vif-APOBEC3G axis inhibitor. *ACS Med. Chem. Lett.* **2012**, *3*, 465–469.
- (10) Nathans, R.; Cao, H.; Sharova, N.; Ali, A.; Sharkey, M.; Stranska, R.; Stevenson, M.; Rana, T. M. Small-molecule inhibition of HIV-1 Vif. *Nat. Biotechnol.* **2008**, *26*, 1187–1192.
- (11) Meanwell, N. A. Synopsis of some recent tactical application of bioisosterism in drug design. *J. Med. Chem.* **2011**, *54*, 2529–2591.

(12) Ko, E.; Liu, J.; Perez, L. M.; Lu, G.; Schaefer, A.; Burgess, K. Universal peptidomimetics. *J. Am. Chem. Soc.* **2011**, *133*, 462–477.

(13) Borg, S.; Vollinga, R. C.; Labarre, M.; Payza, K.; Terenius, L.; Luthman, K. Design, synthesis, and evaluation of Phe-Gly mimetics: heterocyclic building blocks of pseudopeptides. *J. Med. Chem.* **1999**, *42*, 4331–4342.

(14) Valverde, I. E.; Bauman, A.; Kluba, C. A.; Vomstein, S.; Walter, M. A.; Mindt, T. L. 1,2,3-Triazoles as amide bond mimics: triazole scan yields protease-resistant peptidomimetics for tumor targeting. *Angew. Chem., Int. Ed.* **2013**, *52*, 8957–8960.

(15) Tam, A.; Arnold, U.; Soellner, M. B.; Raines, R. T. Protein prosthesis: 1,5-disubstituted[1,2,3]triazoles as cis-peptide bond surrogates. *J. Am. Chem. Soc.* **2007**, *129*, 12670–12671.

(16) Sperotto, E.; van Klink, G. P. M.; de Vries, J. G.; van Koten, G. Ligand-free copper-catalyzed C-S coupling of aryl iodides and thiols. *J. Org. Chem.* **2008**, *73*, 5625–5628.

(17) (a) Liang, G.-B.; Feng, D. D. An improved oxadiazole synthesis using peptide coupling reagents. *Tetrahedron Lett.* **1996**, *37*, 6627–6630. (b) Kumar, D.; Patel, G.; Johnson, E. O.; Shah, K. Synthesis and anticancer activities of novel 3,5-disubstituted-1,2,4-oxadiazoles. *Bioorg. Med. Chem. Lett.* **2009**, *19*, 2739–2741.

(18) Sonogashira, K.; Tohda, Y.; Hagihara, N. A convenient synthesis of acetylenes: catalytic substitutions of acetylenic hydrogen with bromoalkenes, iodoarenes and bromopyridines. *Tetrahedron Lett.* **1975**, *16*, 4467–4470.

(19) Tao, C.-Z.; Cui, X.; Li, J.; Liu, A.-X.; Liu, L.; Guo, Q.-X. Copper-catalyzed synthesis of aryl azides and 1-aryl-1,2,3-triazoles from boronic acids. *Tetrahedron Lett.* **2007**, *48*, 3525–3529.

(20) Rostovtsev, V. V.; Green, L. G.; Fokin, V. V.; Sharpless, K. B. A stepwise Huisgen cycloaddition process: copper(I)-catalyzed regioselective “ligation” of azides and terminal alkynes. *Angew. Chem., Int. Ed.* **2002**, *41*, 2596–2599.

(21) Zhang, L.; Chen, X.; Xue, P.; Sun, H. H. Y.; Williams, I. D.; Sharpless, K. B.; Fokin, V. V.; Jia, G. Ruthenium-catalyzed cycloaddition of alkynes and organic azides. *J. Am. Chem. Soc.* **2005**, *127*, 15998–15999.

(22) Tron, G. C.; Pirali, T.; Billington, R. A.; Canonico, P. L.; Sorba, G.; Genazzani, A. A. Click chemistry reactions in medicinal chemistry: applications of the 1,3-dipolar cycloaddition between azides and alkynes. *Med. Res. Rev.* **2008**, *28*, 278–308.